COMPUTATIONAL INFRASTRUCTURE FOR GEODYNAMICS (CIG)
PRINCETON UNIVERSITY (USA)
CNRS, INRIA and UNIVERSITY OF PAU (FRANCE)

SPECFEM 2D

User Manual
Version 7.0

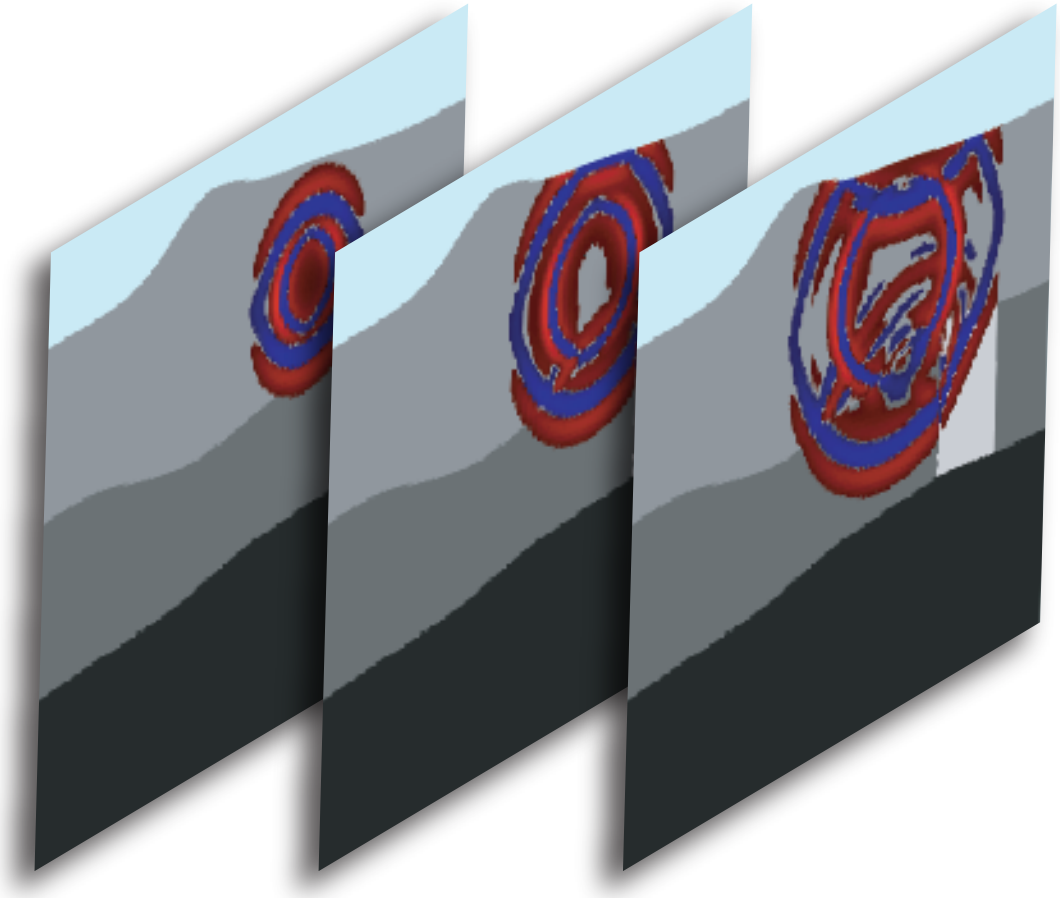

SPECFEM2D
User Manual

Version 7.0

March 13, 2013

Authors

The SPECFEM2D package was first developed by Dimitri Komatitsch and Jean-Pierre Vilotte at IPG in Paris (France) from 1995 to 1997 and then by Dimitri Komatitsch at Harvard University (USA), Caltech (USA) and then CNRS and University of Pau (France) from 1998 to 2005.

Since then it has been developed and maintained by a development team: in alphabetical order, Paul Cristini, Dimitri Komatitsch, Jesús Labarta, Nicolas Le Goff, Pieyre Le Loher, Qinya Liu, Roland Martin, René Matzen, Christina Morency, Daniel Peter, Carl Tape, Jeroen Tromp, Jean-Pierre Vilotte, Zhinan Xie.

Contents

Chapter 1

Introduction

SPECFEM2D facilitates 2D simulations of acoustic, (an)elastic, and poroelastic seismic wave propagation. The 2D spectral-element solver accommodates regular and unstructured meshes, generated for example by Cubit (`http://cubit.sandia.gov`), Gmsh (`http://geuz.org/gmsh`) or GiD (`http://www.gid.cimne.upc.es`). Even mesh creation packages that generate triangles, for instance Delaunay-Voronoi triangulation codes, can be used because each triangle can then easily be decomposed into three quadrangles by linking the barycenter to the center of each edge; while this approach does not generate quadrangles of optimal quality, it can ease mesh creation in some situations and it has been shown that the spectral-element method can very accurately handle distorted mesh elements.

With version 7.0, the 2D spectral-element solver accommodates Convolution PML absorbing layers and well as higher-order time schemes (4th order Runge-Kutta and LDDRK4-6). Convolution or Auxiliary Differential Equation Perfectly Matched absorbing Layers (C-PML or ADE-PML) are described in Komatitsch and Martin [2007], Martin et al. [2008b,c], Martin and Komatitsch [2009], Martin et al. [2010].

The solver has adjoint capabilities and can calculate finite-frequency sensitivity kernels [Tromp et al., 2008, Peter et al., 2011] for acoustic, (an)elastic, and poroelastic media. The package also considers 2D SH and P-SV wave propagation. Finally, the solver can run both in serial and in parallel. See SPECFEM2D (`http://www.geodynamics.org/cig/software/packages/seismo/specfem2d`) for the source code.

The SEM is a continuous Galerkin technique [Tromp et al., 2008, Peter et al., 2011], which can easily be made discontinous [Bernardi et al., 1994, Chaljub, 2000, Kopriva et al., 2002, Chaljub et al., 2003, Legay et al., 2005, Kopriva, 2006, Wilcox et al., 2010, Acosta Minolia and Kopriva, 2011]; it is then close to a particular case of the discontinuous Galerkin technique [Reed and Hill, 1973, Arnold, 1982, Falk and Richter, 1999, Hu et al., 1999, Cockburn et al., 2000, Giraldo et al., 2002, Rivière and Wheeler, 2003, Monk and Richter, 2005, Grote et al., 2006, Ainsworth et al., 2006, Bernacki et al., 2006, Dumbser and Käser, 2006, De Basabe et al., 2008, de la Puente et al., 2009, Wilcox et al., 2010, De Basabe and Sen, 2010, Étienne et al., 2010], with optimized efficiency because of its tensorized basis functions [Wilcox et al., 2010, Acosta Minolia and Kopriva, 2011]. In particular, it can accurately handle very distorted mesh elements [Oliveira and Seriani, 2011].

It has very good accuracy and convergence properties [Maday and Patera, 1989, Seriani and Priolo, 1994, Deville et al., 2002, Cohen, 2002, De Basabe and Sen, 2007, Seriani and Oliveira, 2008]. The spectral element approach admits spectral rates of convergence and allows exploiting hp-convergence schemes. It is also very well suited to parallel implementation on very large supercomputers [Komatitsch et al., 2003, Tsuboi et al., 2003, Komatitsch et al., 2008, Carrington et al., 2008, Komatitsch et al., 2010b] as well as on clusters of GPU accelerating graphics cards [Komatitsch et al., 2009, 2010a, Komatitsch, 2011]. Tensor products inside each element can be optimized to reach very high efficiency [Deville et al., 2002], and mesh point and element numbering can be optimized to reduce processor cache misses and improve cache reuse [Komatitsch et al., 2008]. The SEM can also handle triangular (in 2D) or tetrahedral (in 3D) elements [Wingate and Boyd, 1996, Taylor and Wingate, 2000, Komatitsch et al., 2001, Cohen, 2002, Mercerat et al., 2006] as well as mixed meshes, although with increased cost and reduced accuracy in these elements, as in the discontinuous Galerkin method.

Note that in many geological models in the context of seismic wave propagation studies (except for instance for fault dynamic rupture studies, in which very high frequencies or supershear rupture need to be modeled near the fault, see e.g. Benjemaa et al. [2007, 2009], de la Puente et al. [2009], Tago et al. [2010]) a continuous formulation is sufficient because material property contrasts are not drastic and thus conforming mesh doubling bricks can efficiently handle mesh size variations [Komatitsch and Tromp, 2002, Komatitsch et al., 2004, Lee et al., 2008, 2009a,b].

For a detailed introduction to the SEM as applied to regional seismic wave propagation, please consult Peter et al. [2011], Tromp et al. [2008], Komatitsch and Vilotte [1998], Komatitsch and Tromp [1999], Chaljub et al. [2007] and in particular Lee et al. [2009b,a, 2008], Godinho et al. [2009], van Wijk et al. [2004], Komatitsch et al. [2004]. A detailed theoretical analysis of the dispersion and stability properties of the SEM is available in Cohen [2002], De Basabe and Sen [2007], Seriani and Oliveira [2007] and Seriani and Oliveira [2008].

The SEM was originally developed in computational fluid dynamics [Patera, 1984, Maday and Patera, 1989] and has been successfully adapted to address problems in seismic wave propagation. Early seismic wave propagation applications of the SEM, utilizing Legendre basis functions and a perfectly diagonal mass matrix, include Cohen et al. [1993], Komatitsch [1997], Faccioli et al. [1997], Casadei and Gabellini [1997], Komatitsch and Vilotte [1998] and Komatitsch and Tromp [1999], whereas applications involving Chebyshev basis functions and a nondiagonal mass matrix include Seriani and Priolo [1994], Priolo et al. [1994] and Seriani et al. [1995].

All SPECFEM2D software is written in Fortran2003 with full portability in mind, and conforms strictly to the Fortran2003 standard. It uses no obsolete or obsolescent features of Fortran. The package uses parallel programming based upon the Message Passing Interface (MPI) [Gropp et al., 1994, Pacheco, 1997].

The next release of the code will include support for GPU graphics card acceleration [Komatitsch et al., 2009, 2010a, Michéa and Komatitsch, 2010, Komatitsch, 2011].

1.1 Citation

If you use this code for your own research, please cite at least one article written by the developers of the package, for instance:
Tromp et al. [2008], Peter et al. [2011] or Vai et al. [1999], Lee et al. [2009a, 2008, 2009b], Komatitsch et al. [2010a, 2009], Liu et al. [2004], Chaljub et al. [2007], Komatitsch and Vilotte [1998], Komatitsch and Tromp [1999], Komatitsch et al. [2004], Morency and Tromp [2008] and/or other articles from `http://komatitsch.free.fr/publications.html`

If you use the kernel capabilities of the code, please cite at least one article written by the developers of the package, for instance:
Tromp et al. [2008], Peter et al. [2011], Liu and Tromp [2006], Morency et al. [2009]

If you use the SCOTCH / CUBIT non-structured capabilities, please also cite:
Martin et al. [2008a]

The corresponding BibTeX entries may be found in file `doc/USER_MANUAL/bibliography.bib`.

1.2 Support

This material is based upon work supported by the USA National Science Foundation under Grants No. EAR-0406751 and EAR-0711177, by the French CNRS, French INRIA Sud-Ouest MAGIQUE-3D, French ANR NUMASIS under Grant No. ANR-05-CIGC-002, and European FP6 Marie Curie International Reintegration Grant No. MIRG-CT-2005-017461. Any opinions, findings, and conclusions or recommendations expressed in this material are those of the

authors and do not necessarily reflect the views of the USA National Science Foundation, CNRS, INRIA, ANR or the European Marie Curie program.

Chapter 2

Getting Started

The SPECFEM2D software package comes in a gzipped tar ball. In the directory in which you want to install the package, type

```
tar -zxvf SPECFEM2D_7.0.0.tar.gz
```

The directory `SPECFEM2D-7.0.0/` will then contain the source code. In the following, we will refer to this directory as the root directory `SPECFEM2D/`.

We recommend that you add `ulimit -S -s unlimited` to your `.bash_profile` file and/or `limit stacksize unlimited` to your `.cshrc` file to suppress any potential limit to the size of the Unix stack.

Then, to configure the software for your system, run the `configure` shell script. This script will attempt to guess the appropriate configuration values for your system. However, at a minimum, it is recommended that you explicitly specify the appropriate command names for your Fortran compiler:

```
./configure FC=ifort
```

If you want to run in parallel, i.e., using more than one processor core, then you would type

```
./configure FC=ifort MPIFC=mpif90 --with-mpi
```

Before running the `configure` script, you should probably edit file `flags.guess` to make sure that it contains the best compiler options for your system. Known issues or things to check are:

`Intel ifort compiler` See if you need to add `-assume byterecl` for your machine.

`IBM compiler` See if you need to add `-qsave` or `-qnosave` for your machine.

`Mac OS` You will probably need to install `XCODE`. In addition, the `clock_gettime` routine, which is used by the `SCOTCH` library that we use, does not exist in Mac OS. You will need to replace it with `clock_get_time` if you want to use `SCOTCH`.

The SPECFEM2D software package relies on the SCOTCH library to partition meshes. The SCOTCH library [Pellegrini and Roman, 1996] provides efficent static mapping, graph and mesh partitioning routines. SCOTCH is a free software package developed by François Pellegrini et al. from LaBRI and INRIA in Bordeaux, France, downloadable from the web page `https://gforge.inria.fr/projects/scotch/`. In case no SCOTCH libraries can be found on the system, the configuration will bundle the version provided with the source code for compilation. The path to an existing SCOTCH installation can to be set explicitly with the option `--with-scotch-dir`. Just as an example:

```
./configure FC=ifort MPIFC=mpif90 --with-mpi --with-scotch-dir=/opt/scotch
```

If you use the Intel ifort compiler to compile the code, we recommend that you use the Intel icc C compiler to compile Scotch, i.e., use:

```
./configure CC=icc FC=ifort MPIFC=mpif90
```

For further details about the installation of SCOTCH, go to subdirectory `scotch_5.1.11/` and read `INSTALL.txt`. You may want to download more recent versions of SCOTCH in the future from (`http://www.labri.fr/perso/pelegrin/scotch/scotch_en.html`) . Support for the METIS graph partitioner has been discontinued because SCOTCH is more recent and performs better.

Edit the `Makefile` for more specific modifications. Especially, there are several options available :
`-DUSE_MPI` compiles with use of an MPI library.
`-DUSE_SCOTCH` enables use of graph partitioner SCOTCH.

After these steps, go back to the main directory of SPECFEM2D/ and type

```
make
```

to create all executables which will be placed into the folder `./bin/`.

If you run very large meshes on a relatively small number of processors, the memory size needed on each processor might become greater than 2 gigabytes, which is the upper limit for 32-bit addressing. In this case, on some compilers you may need to add "`-mcmodel=medium`" or "`-mcmodel=medium -shared-intel`" to the configure options of CFLAGS, FCFLAGS and LDFLAGS otherwise the compiler will display an error message (for instance "`relocation truncated to fit: R_X86_64_PC32 against .bss`" or something similar); on an IBM machine with the `xlf` and `xlc` compilers, using `-q64` is usually sufficient.

By default, the solver runs in single precision. This is fine for most application, but if for some reason you want to run the solver in double precision, run the `configure` script with option "`-enable-double-precision`". Keep in mind that this will of course double total memory size and will also make the solver around 20 to 30% slower on many processors.

2.1 Visualizing the subroutine calling tree of the source code

Packages such as `doxywizard` can be used to visualize the subroutine calling tree of the source code. `Doxywizard` is a GUI front-end for configuring and running `doxygen`.

Chapter 3

Mesh Generation

3.1 How to use SPECFEM2D

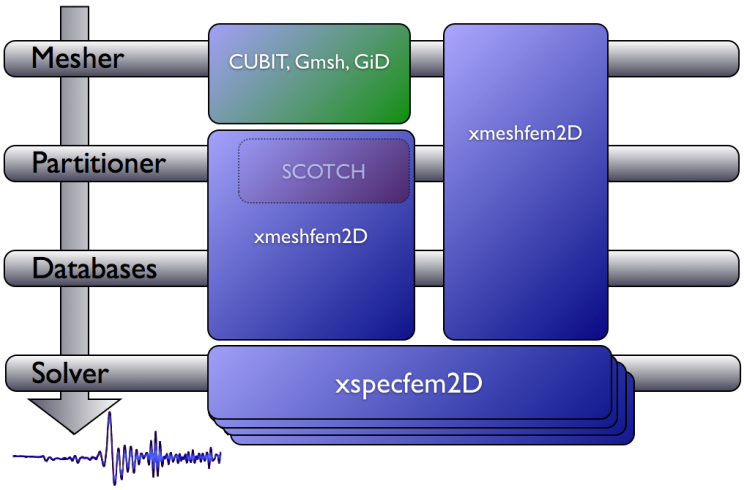

Figure 3.1: Schematic workflow for a SPECFEM2D simulation. The executable `xmeshfem2D` creates the GLL mesh points and assigns specific model parameters. The executable `xspecfem2D` solves the seismic wave propagation.

To run the mesher, please follow these steps:

- edit the input file `DATA/Par_file`, which describes the simulation. The default `DATA/Par_file` provided with the code contains detailed comments and should be almost self-explanatory (note that older `DATA/Par_file` files provided in the `EXAMPLES` directory work fine but some of the comments they contain may be obsolete or even wrong; thus refer to the default `DATA/Par_file` instead for reliable explanations). If you need more details we do not have a detailed description of all the parameters for the 2D version in this manual but you can find useful information in the manuals of the 3D versions, since many parameters and the general philosophy is similar. They are available at (`http://geodynamics.org/wsvn/cig/seismo/3D`) in subdirectories `USER_MANUAL/`. To create acoustic (fluid) regions, just set the S wave speed to zero and the code will see that these elements are fluid and switch to the right equations there automatically, and automatically match them with the solid regions
- if you are using an external mesher (like GID or CUBIT), you should set `read_external_mesh` to `.true.`:

mesh_file is the file describing the mesh : first line is the number of elements, then a list of 4 nodes (quadrilaterals only) forming each elements on each line.

nodes_coords_file is the file containing the coordinates (x and z) of each node: number of nodes on the first line, then coordinates x and z on each line.

materials_file is the number of the material for every elements : an integer ranging from 1 to nbmodels on each line.

free_surface_file is the file describing the edges forming the acoustic free surface: number of edges on the first line, then on each line: number of the element, number of nodes forming the free surface (1 for a point, 2 for an edge), the nodes forming the free surface for this element. If you do not want any free surface, just put 0 on the first line.

absorbing_surface_file is the file describing the edges forming the absorbing boundaries: number of edges on the first line, then on each line: number of the element, number of nodes forming the absorbing edge (must always be equal to 2), the two nodes forming the absorbing edge for this element, and then the type of absorbing edge: 1 for BOTTOM, 2 for RIGHT, 3 for TOP and 4 for LEFT. Only two nodes per element can be listed, i.e., the second parameter of each line must always be equal to 2. If one of your elements has more than one edge along a given absorbing contour (e.g., if that contour has a corner) then list it twice, putting the first edge on the first line and the second edge on the second line. Do not list the same element with the same absorbing edge twice or more, otherwise absorption will not be correct because the edge integral will be improperly subtracted several times. If one of your elements has a single point along the absording contour rather than a full edge, do NOT list it (it would have no weight in the contour integral anyway because it would consist of a single point). If you use 9-node elements, list only the first and last points of the edge and not the intermediate point located around the middle of the edge; the right 9-node curvature will be restored automatically by the code.

tangential_detection_curve_file contains points describing the envelope, used for `source_normal_to_surfa` and `rec_normal_to_surface`. Should be fine grained, and ordained clockwise. Number of points on the first line, then (x,z) coordinates on each line.

- if you have compiled with MPI, you must specify the number of processes.

Then type

```
./bin/xmeshfem2D
```

to create the mesh (which will be stored in directory `OUTPUT_FILES/`). `xmeshfem2D` is serial; it will output several files called `Database??????`, one for each process.

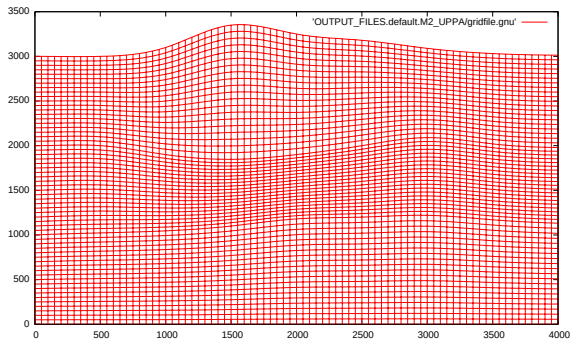

Figure 3.2: Example of a grid file generated by `xmeshfem2D` and visualized with gnuplot (within gnuplot, type ‘`plot "OUTPUT_FILES/gridfile.gnu" w l`‘).

Regarding mesh point numbering in the files created by the mesher, we use the classical convention of 4-node and 9-node finite elements:

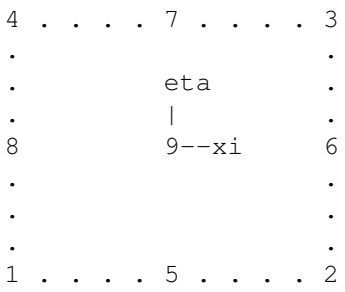

the local coordinate system being ξ and η (`xi` and `eta`). Note that this convention is used to describe the geometry only. In the solver the wave field is then described based on high-order Lagrange interpolants at Gauss-Lobatto-Legendre points, as is classical in spectral-element methods.

3.2 How to use Gmsh to generate an external mesh

Gmsh[1] is a 3D finite element grid generator which can be used for the generation of quadrangle and hexahedral meshes. It is therefore a good candidate for generating meshes which can be processed by SPECFEM2D. Only two modules of Gmsh are of interest for the SPECFEM2D users : the geometry and the mesh modules. An example is given in directory `EXAMPLES/Gmsh_example` which illustrates the generation of an external mesh using these two modules. The model, which is considered, consists of a homogeneous square containing two circles filled with a different material.

The geometry is generated by loading file `SqrCirc.geo` into Gmsh. The end of the `.geo` file contains several lines which are required in order to define the sides of the box and the media. This is done using the following conventions :

```
Physical Line("Top") = {1}; line corresponding to the top of the box
Physical Line("Left") = {2}; line corresponding to the left side of the box
Physical Line("Bottom") = {3}; line corresponding to the bottom of the box
Physical Line("Right") = {4}; line corresponding to the right side of the box
Physical Surface("M1") = {10}; surrounding medium
Physical Surface("M2") = {11,12}; interior of the two circles
```

For instance, if you want to fill the two circles with two different materials, you will have to write :

```
Physical Surface("M1") = {10}; surrounding medium
Physical Surface("M2") = {11}; interior of the big circle
Physical Surface("M3") = {12}; interior of the small circle
```

and, consequently, you will have to define a new medium numbered `3` in the `Par_file`.

Then, a 2D mesh can be created and saved after selecting the appropriate options in Gmsh : `All quads` in `Subdivision algorithm` and `1` or `2` in `Element order` whether you want a 4 or 9 node mesh. This operation will generate a `SqrCirc.msh` file which must be processed to get all the files required by SPECFEM2D when using an external mesh (see previous section). This is done by running a python script called LibGmsh2Specfem.py, located in directory UTILS/Gmsh:

```
python LibGmsh2Specfem.py SqrCirc -t A -b A -r A -l A
```

Where the options `-t`, `-b`, `-r` and `-l` represent the different sides of the model (top, bottom, right and left) and can take the values `A` or `F` if the corresponding side is respectively absorbing or free. All boundaries are absorbing by default. The connections of the generated filenames to the filenames indicated in the previous section are :

- `Mesh_SqrCirc` is the **`mesh_file`**
- `Material_SqrCirc` is the **`material_file`**
- `Nodes_SqrCirc` is the **`nodes_coords_file`**

[1] freely available at the following address : http://www.geuz.org/gmsh/

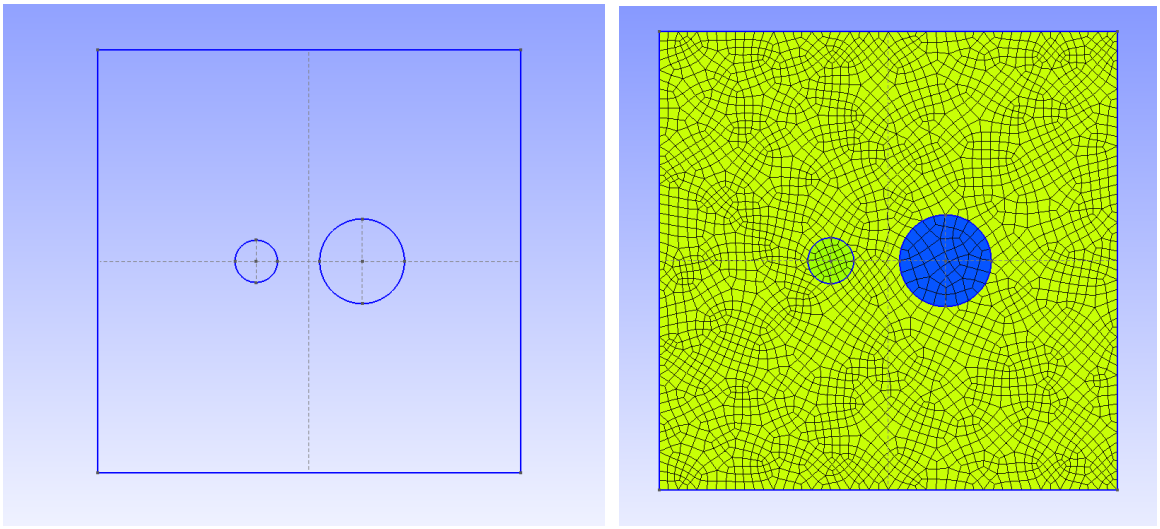

Figure 3.3: Geometry and mesh of the two circle model generated with Gmsh

- `Surf_abs_SqrCirc` is the **`absorbing_surface_file`**
- `Surf_free_SqrCirc` is the **`free_surface_file`**

In addition, four files like `free_surface_file` corresponding to the sides of the model are generated.

If you use CPML, an additional file listing the CPML elements is needed. Its first line is the total number of CPML elements, and then a list of all the CPML elements, one per line. The format of these lines is: in the first column the CPML element number, and in the second column a flag as follows:

Table 3.1: Definition of flags for CPML elements

Flag	Meaning
1	element belongs to a left CPML layer only
2	element belongs to a right CPML layer only
3	element belongs to a bottom CPML layer
4	element belongs to a top CPML layer only
5	element belongs to a top-left CPML corner
6	element belongs to a top-right CPML corner
7	element belongs to a bottom-left CPML corner
8	element belongs to a bottom-right CPML corner

If you use PML and an external velocity and density model (for instance setting flag "READ_EXTERNAL_SEP_FILE" to .true.), you should be careful because mathematically a PML cannot handle heterogeneities along the normal to the PML edge inside the PML layer. This comes from the fact that the damping profile that is defined assumes a constant velocity and density model along the normal direction.

Thus, you need to modify your velocity and density model in order for it to be 1D inside the PML, as shown in Figure 3.4.

This applies to the bottom layer as well; there you should make sure that your model is 1D and thus constant along the vertical direction.

To summarize, only use a 2D velocity and density model inside the physical region, and in all the PML layers extend it by continuity from its values along the inner PML edge.

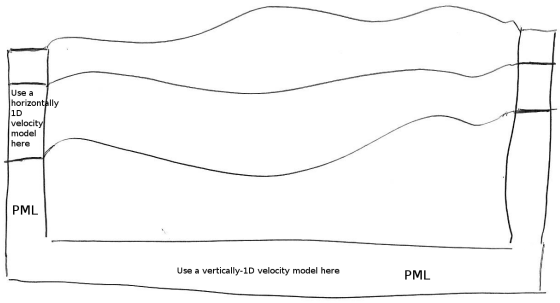

Figure 3.4: How to modify your external 2D velocity and density model in order to use PML. Such a modification is not needed when using Stacey absorbing boundary conditions (but such conditions are significantly less efficient).

3.3 Controlling the quality of an external mesh

To examine the quality of the elements in your externally build mesh, type

```
./bin/xcheck_quality_external_mesh
```

(and answer "3" to the first question asked). This code will tell you which element in the whole mesh has the worst quality (maximum skewness, i.e. maximum deformation of the element angles) and it should be enough to modify this element with the external software package used for the meshing, and to repeat the operation until the maximum skewness of the whole mesh is less or equal to about 0.75 (above is dangerous: from 0.75 to 0.80 could still work, but if there is a single element above 0.80 the mesh should be improved).

The code also shows a histogram of 20 classes of skewness which tells how many element are above the skewness = 0.75, and to which percentage of the total this amounts. To see this histogram, you could type:

```
gnuplot plot_mesh_quality_histogram.gnu
```

This tool is useful to estimate the mesh quality and to see it evolve along the successive corrections.

3.4 Controlling how the mesh samples the wave field

To examine (using Gnuplot) how the mesh samples the wave field, type

```
gnuplot plot_points_per_wavelength_histogram.gnu
```

and also check the following histogram printed on the screen or in the output file:

```
histogram of min number of points per S wavelength (P wavelength in
acoustic regions)
(too small:  poor resolution of calculations - too big = wasting
memory and CPU time)
(threshold value is around 4.5 points per wavelength in elastic media
and 5.5 in acoustic media)
```

If you see that you have a significant number of mesh elements below the threshold indicated, then your simulations will not be accurate and you should create a denser mesh. Conversely, if you have a significant number of mesh elements above the threshold indicated, the mesh your created is too dense, it will be extremely accurate but the simulations will be slow; using a coarser mesh would be sufficient and would lead to faster simulations.

Chapter 4

Running the Solver xspecfem2D

To run the solver, type:

```
./bin/xspecfem2D
```

to run the main solver (use `mpirun` or equivalent if you compiled with parallel support). This will output the seismograms and snapshots of the wave fronts at different time steps in directory `OUTPUT_FILES/`. To visualize them, type "`gs OUTPUT_FILES/vect*.ps`" to see the Postscript files (in which the wave field is represented with small arrows, fluid/solid matching interfaces with a thick pink line, and absorbing edges with a thick green line) and "`gimp OUTPUT_FILES/image*.gif`" to see the color snapshot showing a pixelized image of one of the two components of the wave field (or pressure, depending on what you have selected for the output in `DATA/Par_file`).

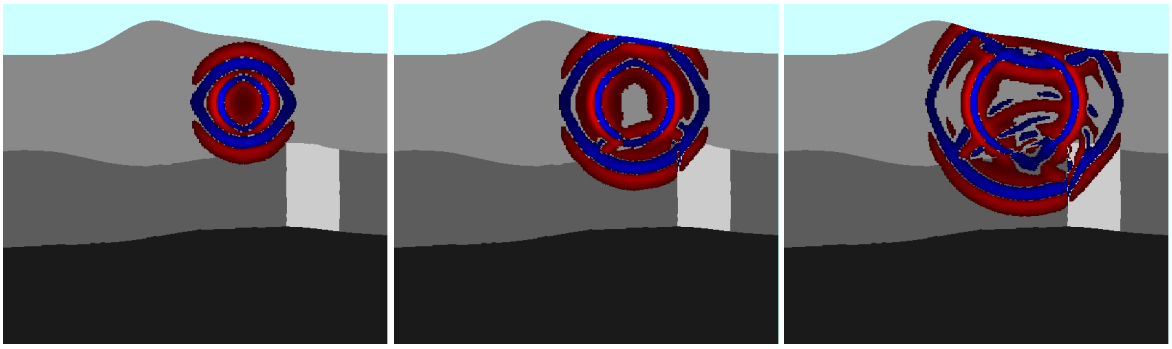

Figure 4.1: Wavefield snapshots of the default example generated by `xspecfem2D` when parameter `output_color_image` is set to `.true.`. To create smaller (subsampled) images you can change double precision parameter `factor_subsample_image = 1.0` to a higher value in file `DATA/Par_file`. This can be useful in the case of very large models. The number of pixels of the image in each direction must be smaller than parameter `NX_NZ_IMAGE_MAX` defined in file `SETUP/constants.h.in`, again to avoid creating huge images in the case of very large models.

Please consider these following points, when running the solver:

- the `DATA/Par_file` given with the code works fine, you can use it without any modification to test the code
- the seismograms `OUTPUT_FILES/*.sem*` are simple ASCII files with two columns: time in the first column and amplitude in the second, therefore they can be visualized with any tool you like, for instance "`gnuplot`"
- if you set flag `assign_external_model` to `.true.` in `DATA/Par_file`, the velocity and density model that is given at the end of `DATA/Par_file` is then ignored and overwritten by the external velocity and density model that you define yourself in `define_external_model.f90`
- when compiling with Intel ifort, use "`-assume byterecl`" option to create binary PNM images displaying the wave field

- there are a few useful scripts and Fortran routines in directory `UTILS/`.
- if you find bugs (or if you have comments or suggestions) please send an email to cig-seismo AT geodynamics.org and the developers will try to fix them and send you an updated version
- you can find a Fortran code to compute the analytical solution for simple media that we use as a reference in benchmarks in many of our articles at (`http://www.spice-rtn.org/library/software/EX2DDIR`). That code is described in: Berg et al. [1994]

The `SOURCE` file located in the `DATA/` directory should be edited in the following way:

source_surf Set this flag to `.true.` to force the source to be located at the surface of the model, otherwise the source will be placed inside the medium

xs source location x in meters

zs source location z in meters

source_type Set this value equal to `1` for elastic forces or acoustic pressure, set this to `2` for moment tensor sources. For a plane wave including converted and reflected waves at the free surface, P wave = 1, S wave = 2, Rayleigh wave = 3; for a plane wave without converted nor reflected waves at the free surface, i.e. the incident wave only, P wave = 4, S wave = 5. (incident plane waves are turned on by parameter `initialfield` in `DATA/Par_file`).

time_function_type Choose a source-time function: set this value to `1` to use a Ricker, `2` the first derivative, `3` a Gaussian, `4` a Dirac or `5` a Heaviside source-time function.

f0 Set this to the dominant frequency of the source. For point-source simulations using a Heaviside source-time function (time_function_type "5"), we recommend setting the source frequency parameter `f0` equal to a high value, which corresponds to simulating a step source-time function, i.e., a moment-rate function that is a delta function.

The `half duration` of a source is obtained by `1/f0`. If the code will use a Gaussian source-time function (time_function_type "3") (i.e., a signal with a shape similar to a 'smoothed triangle', as explained in Komatitsch and Tromp [2002] and shown in Fig 4.2), the source-time function uses a half-width of `half duration`. We prefer to run the solver with `half duration` set to zero and convolve the resulting synthetic seismograms in post-processing after the run, because this way it is easy to use a variety of source-time functions. Komatitsch and Tromp [2002] determined that the noise generated in the simulation by using a step source time function may be safely filtered out afterward based upon a convolution with the desired source time function and/or low-pass filtering. Use the serial code `convolve_source_timefunction.f90` and the script `convolve_source_timefunction.csh` for this purpose, or alternatively use signal-processing software packages such as SAC (`www.llnl.gov/sac`). Type

```
make convolve_source_timefunction
```

to compile the code and then set the parameter `hdur` in `convolve_source_timefunction.csh` to the desired half-duration.

t0 For single sources, we recommend to set the time shift parameter `t0` equal to 0.0. The time shift parameter would simply apply an overall time shift to the synthetics (according to the time shift of the first source), something that can be done in the post-processing. This time shift parameter can be non-zero when using multiple sources.

anglesource angle of the source (for a force only); for a plane wave, this is the incidence angle. For moment tensor sources this parameter is unused.

Mxx,Mzz,Mxz Moment tensor components (valid only for moment tensor sources, source_type "2"). Note that the units for the components of a moment tensor source are different in SPECFEM2D and in SPECFEM3D:

SPECFEM3D: in SPECFEM3D the moment tensor components are in dyne*cm

SPECFEM2D: in SPECFEM2D the moment tensor components are in N*m

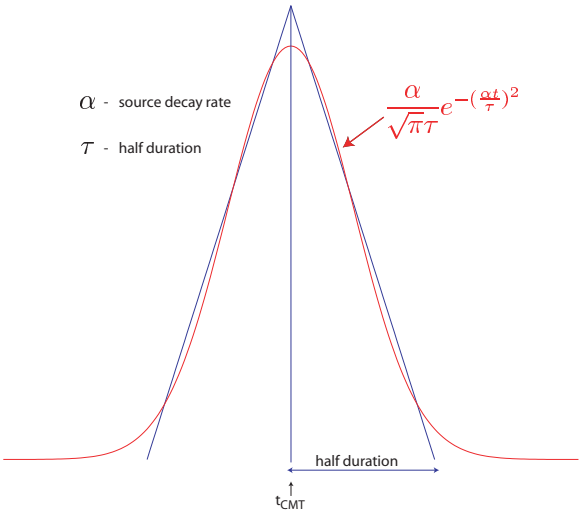

Figure 4.2: Comparison of the shape of a triangle and the Gaussian function actually used.

factor amplification factor

Note, the zero time of the simulation corresponds to the center of the triangle/Gaussian, or the centroid time of the earthquake. The start time of the simulation is $t = -1.2 * \texttt{half duration} + \texttt{t0}$ (the factor 1.2 is to make sure the moment rate function is very close to zero when starting the simulation; Heaviside functions use a factor 2.0), the half duration is obtained by 1/f0. If you prefer, you can fix this start time by setting the parameter `USER_T0` in the `constants.h` file to a positive, non-zero value. The simulation in that case would start at a starting time equal to `-USER_T0`.

Caution

See file `todo_list_please_dont_remove.txt` for a list of known bugs, problems, or missing options.

Coupled Simulations

The code supports acoustic/elastic, acoustic/poroelastic, elastic/poroelastic, and acoustic,elastic/poroelastic simulations.

Elastic/poroelastic coupling supports anisotropy, but not attenuation for the elastic material.

4.1 How to run P-SV or SH (membrane) wave simulations

For elastic materials, you have these additional options:

P-SV: To run a P-SV waves calculation propagating in the x-z plane, set `p_sv = .true.` in the `Par_file`.

SH: To run a SH (membrane) waves calculation traveling in the x-z plane with a y-component of motion, set `p_sv = .false.`

This feature is only implemented for elastic materials and sensitivity kernels can be calculated (see Tape et al. [2007] for details on membrane surface waves).

A useful Python script called `SEM_save_dir.py`, written by Paul Cristini from Laboratoire de Mecanique et d'Acoustique, CNRS, Marseille, France, is provided. It allows one to automatically save all the parameters and results of a given simulation.

4.2 How to use anisotropy

Following Carcione et al. [1988], we use the classical reduced Voigt notation [Helbig, 1994, Carcione, 2007]:

The constitutive relation of a heterogeneous anisotropic and elastic solid is expressed by the generalized Hooke's law, which can be written as

$$\sigma_{ij} = c_{ijkl}\varepsilon_{kl}, \qquad i, j, k, l = 1, \ldots, 3,$$

where t is the time, $\mathbf{x}$ is the position vector, $\sigma_{ij}(\mathbf{x}, t)$ and $\varepsilon_{ij}(\mathbf{x}, t)$ are the Cartesian components of the stress and strain tensors respectively, and $c_{ijkl}(\mathbf{x})$ are the components of a fourth-order tensor called the elasticities of the medium. The Einstein convention for repeated indices is used.

To express the stress–strain relation for a transversely isotropic medium we introduce a shortened matrix notation commonly used in the literature. With this convention, pairs of subscripts concerning the elasticities are replaced by a single number according to the following correspondence:

$$(11) \rightarrow 1, \quad (22) \rightarrow 2, \quad (33) \rightarrow 3, \quad (23) = (32) \rightarrow 4,$$
$$(31) = (13) \rightarrow 5, \quad (12) = (21) \rightarrow 6.$$

Thus in the most general 2D case we have the following convention for the stress-strain relationship:

```
! implement anisotropy in 2D
sigma_xx = c11*dux_dx + c15*(duz_dx + dux_dz) + c13*duz_dz
sigma_zz = c13*dux_dx + c35*(duz_dx + dux_dz) + c33*duz_dz
sigma_xz = c15*dux_dx + c55*(duz_dx + dux_dz) + c35*duz_dz
```

where the notations are for instance `duz_dx = d(Uz) / dx`.

4.3 How to use poroelasticity

Check the following new inputs in `Par_file`:

In section **"# geometry of model and mesh description"**:
`TURN_VISCATTENUATION_ON`, `Q0`, and `FREQ0` deal with viscous damping in a poroelastic medium. `Q0` is the quality factor set at the central frequency `FREQ0`. For more details see Morency and Tromp [2008].

In section **"# time step parameters"**:
`SIMULATION_TYPE` defines the type of simulations
(1) forward simulation
(2) UNUSED (purposely, for compatibility with the numbering convention used in our 3D codes)
(3) adjoint method and kernels calculation

In section **"# source parameters"**:
The code now support multi sources. `NSOURCE` is the number of source. Parameters of the sources are displayed in the file `SOURCE`, which must be in the directory `DATA/`. The components of a moment tensor source must be given in N.m, not in dyne.cm as in the `DATA/CMTSOLUTION` source file of the 3D version of the code.

In section **"# receiver line parameters for seismograms"**:
`SAVE_FORWARD` determines if the last frame of a forward simulation is saved (`.true.`) or not (`.false`)

In section **"# define models...."**:
There are three possible types of models:
`I`: (model_number 1 rho Vp Vs 0 0 QKappa Qmu 0 0 0 0 0 0) or
`II`: (model_number 2 rho c11 c13 c15 c33 c35 c55 0 0 0 0 0 0) or
`III`: (model_number 3 rhos rhof phi c kxx kxz kzz Ks Kf Kfr etaf mufr Qmu).

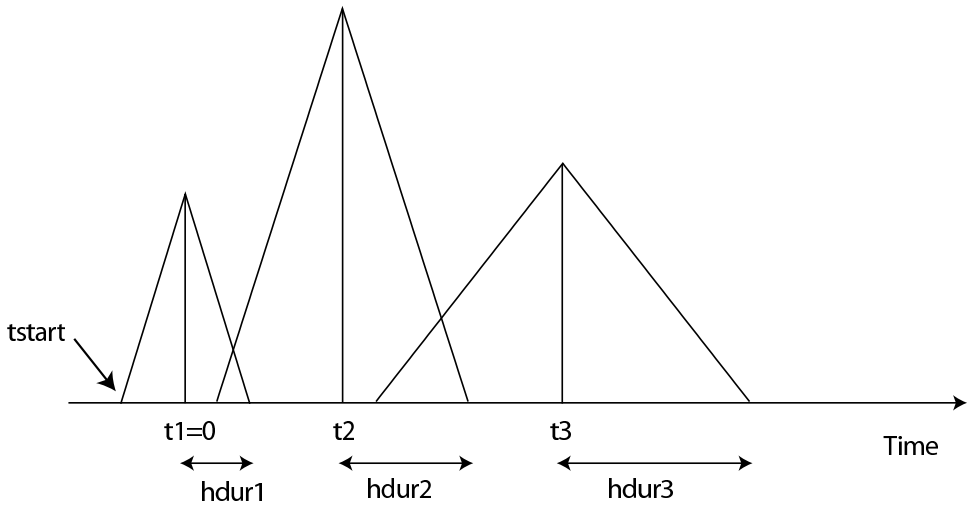

Figure 4.3: Example of timing for three sources. The center of the first source triangle is defined to be time zero. Note that this is NOT in general the hypocentral time, or the start time of the source (marked as tstart). The time shift parameter `t0` in the `SOURCE` file would be t1(=0), t2, t3 in this case, and the half-duration parameter, resp. `f0`, would be hdur1=1/f0_1, hdur2=1/f0_2, hdur3=1/f0_3 for the sources 1, 2, 3 respectively.

For istropic elastic/acoustic material use `I` and set Vs to zero to make a given model acoustic, for anisotropic elastic use `II`, and for isotropic poroelastic material use `III`. The mesh can contain acoustic, elastic, and poroelastic models simultaneously. rho_s = solid density
rho_f = fluid density
phi = porosity
tort = tortuosity
permxx = xx component of permeability tensor
permxz = xz,zx components of permeability tensor
permzz = zz component of permeability tensor
kappa_s = solid bulk modulus
kappa_f= fluid bulk modulus
kappa_fr= frame bulk modulus
eta_f = fluid viscosity
mu_fr = frame shear modulus
Qmu = shear quality factor

Note: for the poroelastic case, mu_s is irrelevant. For details on the poroelastic theory see Morency and Tromp [2008].

`get_poroelastic_velocities.f90` allows to compute cpI, cpII, and cs function of the source dominant frequency. Notice that for this calculation we use permxx and the dominant frequency of the first source , f0(1). Caution if you use several sources with different frequencies and if you consider anistropic permeability.

4.4 How to set plane waves as initial conditions

To simulate propagation of incoming plane waves in the simulation domain, initial conditions based on analytical formulae of plane waves in homogenous model need to be set. No additional body or boundary forces are required. To set up this senario:

`Par_file`:

- switch on `initialfield = .true.`

- at this point setting `add_bielak_condition` does not seem to help with absorbing boundaries, therefore, it should be turned off.

`SOURCE`:

- `zs` has to be the same as the height of the simulation domain defined in `interfacesfile`.
- `xs` is the x-coordinate of the intersection of the initial plane wave front with the free surface.
- `source_type` = 1 for a plane P wave, 2 for a plane SV wave, 3 for a Rayleigh wave.
- `angleforce` can be negative to indicate a plane wave incident from the right (instead of the left)

4.5 How to choose the time step

Three different explicit conditionally-stable time schemes can be used for elastic, acoustic (fluid) or coupled elastic/acoustic media: the Newmark method, the low-dissipation and low-dispersion fourth-order six-stage Runge-Kutta method (LDDRK4-6) presented in Berland et al. [2006], and the classical fourth-order four-stage Runge-Kutta (RK4) method. Currently the last two methods are not implemented for poro-elastic media. According to De Basabe and Sen [2010] and Berland et al. [2006], with different degrees $N = NGLLX - 1$ of the GLL basis funtions the CFL bounds are given in the following tables. Note that by default the SPECFEM solver uses $NGLLX = 5$ and thus a degree $N = 4$, which is thus the value you should use in most cases in the following tables. You can directly compare these values with the value given in sentence 'Max stability for P wave velocity' in file `output_solver.txt` to see whether you set the correct Δ_t in `Par_file` or not. For elastic simulation, the CFL value given in `output_solver.txt` does not consider the Vp/Vs ratio, but the CFL limit slight decreases when Vp/Vs increases. In viscoelastic simulations the CFL limit does not change compared to the elastic case because we use a rational approximation of a constant quality factor Q, which has no attenuation effect on zero-frequency waves. Additionally, if you use C-PML absorbing layers in your simulations, which are implemented for the Newmark and LDDRK4-6 techniques but not for the classical RK4), the CFL upper limit decreases to approximately 95% of the limit without absorbing layers in the case of Newmark and to 85% in the case of LDDRK4-6.

Table 4.1: CFL upper bound for an acoustic (fluid) simulation.

Degree N	Newmark	LDDRK4-6	RK4
1	0.709	1.349	1.003
2	0.577	1.098	0.816
3	0.593	1.129	0.839
4	**0.604**	**1.150**	**0.854**
5	0.608	1.157	0.860
6	0.608	1.157	0.860
7	0.608	1.157	0.860
8	0.607	1.155	0.858
9	0.607	1.155	0.858
10	0.607	1.155	0.858

Table 4.2: CFL upper bound for an elastic simulation with Vp/Vs = $\sqrt{2}$.

Degree N	Newmark	LDDRK4-6	RK4
1	0.816	1.553	1.154
2	0.666	1.268	0.942
3	0.684	1.302	0.967
4	**0.697**	**1.327**	**0.986**
5	0.700	1.332	0.990
6	0.700	1.332	0.990
7	0.700	1.332	0.990
8	0.699	1.330	0.989
9	0.698	1.328	0.987
10	0.698	1.328	0.987

Chapter 5

Adjoint Simulations

5.1 How to obtain Finite Sensitivity Kernels

1. Run a forward simulation:
   => `SIMULATION_TYPE = 1`
   => `SAVE_FORWARD = .true.`
   => `seismotype = 1` (we need to save the displacement fields to later on derive the adjoint source. Note: if the user forgets it, the program corrects it when reading the proper `SIMULATION_TYPE` and `SAVE_FORWARD` combination and a warning message appears in the ouput file)

   Important output files (for example, for the elastic case, P-SV waves):
   s `absorb_elastic_bottom*****.bin`
   `absorb_elastic_left*****.bin`
   `absorb_elastic_right*****.bin`
   `absorb_elastic_top*****.bin`
   `lastframe_elastic*****.bin`
   `S****.AA.BXX.semd`
   `S****.AA.BXZ.semd`

2. Define the adjoint source:
   Use `adj_seismogram.f90`
   Edit to update `NSTEP`, `nrec`, `t0`, `deltat`, and the position of the cut to pic any given phase if needed (`tstart`,`tend`), add the right number of stations, and put one component of the source to zero if needed. The ouput files of `adj_seismogram.f90` are `S****.AA.BXX.adj` and `S****.AA.BXZ.adj`, for P-SV waves (and `S****.AA.BXY.adj`, for SH (membrane) waves). Note that you will need these three files (`S****.AA.BXX.adj`, `S****.AA.BXY.adj` and `S****.AA.BXZ.adj`) to be present in the `SEM/` directory together with the `absorb_elastic_****.bin` and `lastframe_elastic.bin` files to be read when running the adjoint simulation.

3. Run the adjoint simulation:
   Make sure that the adjoint source files absorbing boundaries and last frame files are in the `OUTPUT_FILES/` directory.
   => `SIMULATION_TYPE = 3`
   => `SAVE_FORWARD = .false.`

   Output files (for example for the elastic case):
   `snapshot_rho_kappa_mu*****`
   `snapshot_rhop_alpha_beta*****`

which are the primary moduli kernels and the phase velocities kernels respectively, in ascii format and at the local level, that is as "kernels(i,j,ispec)".

Remarks about adjoint runs and solving inverse problems

SPECFEM2D can produce the gradient of the misfit function for a tomographic inversion, but options for using the gradient within an iterative inversion are left to the user (e.g., conjugate-gradient, steepest descent). The plan is to include some examples in the future.

The algorithm is simple:

1. calculate the forward wave field $\mathbf{s}(x,t)$
2. calculate the adjoint wave field $\mathbf{s}^\dagger(x,t)$
3. calculate their interaction $\mathbf{s}(x,t) \cdot \mathbf{s}^\dagger(x,T-t)$ (these symbolic, temporal and spatial derivatives should be included)
4. integrate the interactions, which is summation in the code.

That is all. Step 3 has some tricks in implementation, but which can be skipped by regular users.

If you look into SPECFEM2D, besides "rhop_ac_kl" and "rho_ac_kl", there are more variables such as "kappa_ac_kl" and "rho_el_kl" etc. "rho" denotes density ρ ("kappa" for bulk modulus κ etc.), "ac" denotes acoustic ("el" for elastic), "kl" means kernel (and you may find "k" as well, which is the interaction at each time step, i.e., before doing time integration).

Caution

Please note that

- at the moment, adjoint simulations do not support anisotropy, attenuation, and viscous damping.
- you will need `S****.AA.BXX.adj`, `S****.AA.BXY.adj` and `S****.AA.BXZ.adj` to be present in directory `SEM/` even if you are just running an acoustic or poroelastic adjoint simulation.
  `S****.AA.BXX.adj` is the only relevant component for an acoustic case.
  `S****.AA.BXX.adj` and `S****.AA.BXZ.adj` are the only relevant components for a poroelastic case.

Chapter 6

Oil and gas industry simulations

The SPECFEM2D package provides compatibilities in industrial (oil and gas industry) types of simulations. These features include importing Seismic Unix (SU) format wavespeed models into SPECFEM2D, outputing seismograms also in SU format with a few key parameters defined in the trace headers and reading adjoint sources in SU format etc. There is one example given in EXAMPLES/INDUSTRIAL_FORMAT, which you can follow.

We also changed the relationship between adjoint potential and adjoint displacement in fluid region (the relationship between forward potential and forward displacement remains the same as previsouly defined). The new definition is critical when there are adjoint sources (in other words, receivers) in the acoustic domain, and is the direct consequence of the optimization problem.

$$\begin{aligned} \mathbf{s} &\equiv \frac{1}{\rho}\,\nabla\phi \\ p &\equiv -\kappa(\nabla\cdot\mathbf{s}) = -\partial_t^2\phi \end{aligned}$$

$$\begin{aligned} \partial_t^2\mathbf{s}^\dagger &\equiv -\frac{1}{\rho}\,\nabla\phi^\dagger \\ p^\dagger &\equiv -\kappa(\nabla\cdot\mathbf{s}^\dagger) = \phi^\dagger \end{aligned}$$

Acknowledgments

The Gauss-Lobatto-Legendre subroutines in `gll_library.f90` are based in part on software libraries from the Massachusetts Institute of Technology, Department of Mechanical Engineering (Cambridge, Massachusetts, USA). The non-structured global numbering software was provided by Paul F. Fischer (Brown University, Providence, Rhode Island, USA, now at Argonne National Laboratory, USA).

Please e-mail your feedback, questions, comments, and suggestions to Jeroen Tromp (`jtromp-AT-princeton.edu`) or to the CIG Computational Seismology Mailing List (`cig-seismo@geodynamics.org`).

Copyright

Main historical authors: Dimitri Komatitsch and Jeroen Tromp
Princeton University, USA, and CNRS / INRIA / University of Pau, France

Bibliography

C. A. Acosta Minolia and D. A. Kopriva. Discontinuous Galerkin spectral element approximations on moving meshes. *J. Comput. Phys.*, 230(5):1876–1902, 2011. doi: 10.1016/j.jcp.2010.11.038.

M. Ainsworth, P. Monk, and W. Muniz. Dispersive and dissipative properties of discontinuous Galerkin finite element methods for the second-order wave equation. *Journal of Scientific Computing*, 27(1):5–40, 2006. doi: 10.1007/s10915-005-9044-x.

D. N. Arnold. An interior penalty finite element method with discontinuous elements. *SIAM Journal on Numerical Analysis*, 19(4):742–760, 1982. doi: 10.1137/0719052.

M. Benjemaa, N. Glinsky-Olivier, V. M. Cruz-Atienza, J. Virieux, and S. Piperno. Dynamic non-planar crack rupture by a finite volume method. *Geophys. J. Int.*, 171(1):271–285, 2007. doi: 10.1111/j.1365-246X.2006.03500.x.

M. Benjemaa, N. Glinsky-Olivier, V. M. Cruz-Atienza, and J. Virieux. 3D dynamic rupture simulation by a finite volume method. *Geophys. J. Int.*, 178(1):541–560, 2009. doi: 10.1111/j.1365-246X.2009.04088.x.

P. Berg, F. If, P. Nielsen, and O. Skovegaard. Analytic reference solutions. In K. Helbig, editor, *Modeling the Earth for oil exploration, Final report of the CEC's GEOSCIENCE I Program 1990-1993*, pages 421–427. Pergamon Press, Oxford, United Kingdom, 1994.

J. Berland, C. Bogey, and C. Bailly. Low-dissipation and low-dispersion fourth-order Runge-Kutta algorithm. *Computers and Fluids*, 35:1459–1463, 2006.

M. Bernacki, S. Lanteri, and S. Piperno. Time-domain parallel simulation of heterogeneous wave propagation on unstructured grids using explicit, nondiffusive, discontinuous Galerkin methods. *J. Comput. Acoust.*, 14(1):57–81, 2006.

C. Bernardi, Y. Maday, and A. T. Patera. A new nonconforming approach to domain decomposition: the Mortar element method. In H. Brezis and J. L. Lions, editors, *Nonlinear partial differential equations and their applications*, Séminaires du Collège de France, pages 13–51, Paris, 1994. Pitman.

J. M. Carcione. *Wave fields in real media: Theory and numerical simulation of wave propagation in anisotropic, anelastic, porous and electromagnetic media*. Elsevier Science, Amsterdam, The Netherlands, second edition, 2007.

J. M. Carcione, D. Kosloff, and R. Kosloff. Wave propagation simulation in an elastic anisotropic (transversely isotropic) solid. *Q. J. Mech. Appl. Math.*, 41(3):319–345, 1988.

L. Carrington, D. Komatitsch, M. Laurenzano, M. Tikir, D. Michéa, N. Le Goff, A. Snavely, and J. Tromp. High-frequency simulations of global seismic wave propagation using SPECFEM3D_GLOBE on 62 thousand processor cores. In *SC'08: Proceedings of the 2008 ACM/IEEE conference on Supercomputing*, SC '08, pages 60:1–60:11, Austin, Texas, USA, Nov. 2008. IEEE Press. doi: 10.1145/1413370.1413432. Article #60, Gordon Bell Prize finalist article.

F. Casadei and E. Gabellini. Implementation of a 3D coupled Spectral Element solver for wave propagation and soil-structure interaction simulations. Technical report, European Commission Joint Research Center Report EUR17730EN, Ispra, Italy, 1997.

E. Chaljub. *Modélisation numérique de la propagation d'ondes sismiques en géométrie sphérique : application à la sismologie globale (Numerical modeling of the propagation of seismic waves in spherical geometry: application to global seismology)*. PhD thesis, Université Paris VII Denis Diderot, Paris, France, 2000.

E. Chaljub, Y. Capdeville, and J. P. Vilotte. Solving elastodynamics in a fluid-solid heterogeneous sphere: a parallel spectral-element approximation on non-conforming grids. *J. Comput. Phys.*, 187(2):457–491, 2003.

E. Chaljub, D. Komatitsch, J. P. Vilotte, Y. Capdeville, B. Valette, and G. Festa. Spectral element analysis in seismology. In R.-S. Wu and V. Maupin, editors, *Advances in wave propagation in heterogeneous media*, volume 48 of *Advances in Geophysics*, pages 365–419. Elsevier - Academic Press, London, UK, 2007.

B. Cockburn, G. E. Karniadakis, and C.-W. Shu. *Discontinuous Galerkin Methods: Theory, Computation and Applications*. Springer, Heidelberg, Germany, 2000.

G. Cohen. *Higher-order numerical methods for transient wave equations*. Springer-Verlag, Berlin, Germany, 2002.

G. Cohen, P. Joly, and N. Tordjman. Construction and analysis of higher-order finite elements with mass lumping for the wave equation. In R. Kleinman, editor, *Proceedings of the second international conference on mathematical and numerical aspects of wave propagation*, pages 152–160. SIAM, Philadelphia, Pennsylvania, USA, 1993.

J. D. De Basabe and M. K. Sen. Grid dispersion and stability criteria of some common finite-element methods for acoustic and elastic wave equations. *Geophysics*, 72(6):T81–T95, 2007. doi: 10.1190/1.2785046.

J. D. De Basabe and M. K. Sen. Stability of the high-order finite elements for acoustic or elastic wave propagation with high-order time stepping. *Geophys. J. Int.*, 181(1):577–590, 2010. doi: 10.1111/j.1365-246X.2010.04536.x.

J. D. De Basabe, M. K. Sen, and M. F. Wheeler. The interior penalty discontinuous Galerkin method for elastic wave propagation: grid dispersion. *Geophys. J. Int.*, 175(1):83–93, 2008. doi: 10.1111/j.1365-246X.2008.03915.x.

J. de la Puente, J. P. Ampuero, and M. Käser. Dynamic rupture modeling on unstructured meshes using a discontinuous Galerkin method. *J. Geophys. Res.*, 114:B10302, 2009. doi: 10.1029/2008JB006271.

M. O. Deville, P. F. Fischer, and E. H. Mund. *High-Order Methods for Incompressible Fluid Flow*. Cambridge University Press, Cambridge, United Kingdom, 2002.

M. Dumbser and M. Käser. An arbitrary high-order discontinuous Galerkin method for elastic waves on unstructured meshes-II. The three-dimensional isotropic case. *Geophys. J. Int.*, 167(1):319–336, 2006. doi: 10.1111/j.1365-246X.2006.03120.x.

V. Étienne, E. Chaljub, J. Virieux, and N. Glinsky. An hp-adaptive discontinuous Galerkin finite-element method for 3-D elastic wave modelling. *Geophys. J. Int.*, 183(2):941–962, 2010. doi: 10.1111/j.1365-246X.2010.04764.x.

E. Faccioli, F. Maggio, R. Paolucci, and A. Quarteroni. 2D and 3D elastic wave propagation by a pseudo-spectral domain decomposition method. *J. Seismol.*, 1:237–251, 1997.

R. S. Falk and G. R. Richter. Explicit finite element methods for symmetric hyperbolic equations. *SIAM Journal on Numerical Analysis*, 36(3):935–952, 1999. doi: 10.1137/S0036142997329463.

F. X. Giraldo, J. S. Hesthaven, and T. Warburton. Nodal high-order discontinuous Galerkin methods for the spherical shallow water equations. *J. Comput. Phys.*, 181(2):499–525, 2002. doi: 10.1006/jcph.2002.7139.

L. Godinho, P. A. Mendes, A. Tadeu, A. Cadena-Isaza, C. Smerzini, F. J. Sánchez-Sesma, R. Madec, and D. Komatitsch. Numerical simulation of ground rotations along 2D topographical profiles under the incidence of elastic plane waves. *Bull. Seismol. Soc. Am.*, 99(2B):1147–1161, 2009. doi: 10.1785/0120080096.

W. Gropp, E. Lusk, and A. Skjellum. *Using MPI, portable parallel programming with the Message-Passing Interface*. MIT Press, Cambridge, USA, 1994.

M. J. Grote, A. Schneebeli, and D. Schötzau. Discontinuous Galerkin finite element method for the wave equation. *SIAM Journal on Numerical Analysis*, 44(6):2408–2431, 2006. doi: 10.1137/05063194X.

K. Helbig. Foundations of anisotropy for exploration seismics. In K. Helbig and S. Treitel, editors, *Handbook of Geophysical exploration, section I: Seismic exploration*, volume 22. Pergamon, Oxford, England, 1994.

F. Q. Hu, M. Y. Hussaini, and P. Rasetarinera. An analysis of the discontinuous Galerkin method for wave propagation problems. *J. Comput. Phys.*, 151(2):921–946, 1999. doi: 10.1006/jcph.1999.6227.

D. Komatitsch. *Méthodes spectrales et éléments spectraux pour l'équation de l'élastodynamique 2D et 3D en milieu hétérogène (Spectral and spectral-element methods for the 2D and 3D elastodynamics equations in heterogeneous media)*. PhD thesis, Institut de Physique du Globe, Paris, France, May 1997. 187 pages.

D. Komatitsch. Fluid-solid coupling on a cluster of GPU graphics cards for seismic wave propagation. *C. R. Acad. Sci., Ser. IIb Mec.*, 339:125–135, 2011. doi: 10.1016/j.crme.2010.11.007.

D. Komatitsch and R. Martin. An unsplit convolutional Perfectly Matched Layer improved at grazing incidence for the seismic wave equation. *Geophysics*, 72(5):SM155–SM167, 2007. doi: 10.1190/1.2757586.

D. Komatitsch and J. Tromp. Introduction to the spectral-element method for 3-D seismic wave propagation. *Geophys. J. Int.*, 139(3):806–822, 1999. doi: 10.1046/j.1365-246x.1999.00967.x.

D. Komatitsch and J. Tromp. Spectral-element simulations of global seismic wave propagation-I. Validation. *Geophys. J. Int.*, 149(2):390–412, 2002. doi: 10.1046/j.1365-246X.2002.01653.x.

D. Komatitsch and J. P. Vilotte. The spectral-element method: an efficient tool to simulate the seismic response of 2D and 3D geological structures. *Bull. Seismol. Soc. Am.*, 88(2):368–392, 1998.

D. Komatitsch, R. Martin, J. Tromp, M. A. Taylor, and B. A. Wingate. Wave propagation in 2-D elastic media using a spectral element method with triangles and quadrangles. *J. Comput. Acoust.*, 9(2):703–718, 2001. doi: 10.1142/S0218396X01000796.

D. Komatitsch, S. Tsuboi, C. Ji, and J. Tromp. A 14.6 billion degrees of freedom, 5 teraflops, 2.5 terabyte earthquake simulation on the Earth Simulator. In *SC'03: Proceedings of the 2003 ACM/IEEE conference on Supercomputing*, SC '03, pages 4–11, Phoenix, Arizona, USA, Nov. 2003. ACM. doi: 10.1145/1048935.1050155. Gordon Bell Prize winner article.

D. Komatitsch, Q. Liu, J. Tromp, P. Süss, C. Stidham, and J. H. Shaw. Simulations of ground motion in the Los Angeles basin based upon the spectral-element method. *Bull. Seismol. Soc. Am.*, 94(1):187–206, 2004. doi: 10.1785/0120030077.

D. Komatitsch, J. Labarta, and D. Michéa. A simulation of seismic wave propagation at high resolution in the inner core of the Earth on 2166 processors of MareNostrum. *Lecture Notes in Computer Science*, 5336:364–377, 2008.

D. Komatitsch, D. Michéa, and G. Erlebacher. Porting a high-order finite-element earthquake modeling application to NVIDIA graphics cards using CUDA. *Journal of Parallel and Distributed Computing*, 69(5):451–460, 2009. doi: 10.1016/j.jpdc.2009.01.006.

D. Komatitsch, G. Erlebacher, D. Göddeke, and D. Michéa. High-order finite-element seismic wave propagation modeling with MPI on a large GPU cluster. *J. Comput. Phys.*, 229(20):7692–7714, 2010a. doi: 10.1016/j.jcp.2010.06.024.

D. Komatitsch, L. P. Vinnik, and S. Chevrot. SHdiff/SVdiff splitting in an isotropic Earth. *J. Geophys. Res.*, 115(B7):B07312, 2010b. doi: 10.1029/2009JB006795.

D. A. Kopriva. Metric identities and the discontinuous spectral element method on curvilinear meshes. *Journal of Scientific Computing*, 26(3):301–327, 2006. doi: 10.1007/s10915-005-9070-8.

D. A. Kopriva, S. L. Woodruff, and M. Y. Hussaini. Computation of electromagnetic scattering with a non-conforming discontinuous spectral element method. *Int. J. Numer. Meth. Eng.*, 53(1):105–122, 2002. doi: 10.1002/nme.394.

S. J. Lee, H. W. Chen, Q. Liu, D. Komatitsch, B. S. Huang, and J. Tromp. Three-dimensional simulations of seismic wave propagation in the Taipei basin with realistic topography based upon the spectral-element method. *Bull. Seismol. Soc. Am.*, 98(1):253–264, 2008. doi: 10.1785/0120070033.

S. J. Lee, Y. C. Chan, D. Komatitsch, B. S. Huang, and J. Tromp. Effects of realistic surface topography on seismic ground motion in the Yangminshan region of Taiwan based upon the spectral-element method and LiDAR DTM. *Bull. Seismol. Soc. Am.*, 99(2A):681–693, 2009a. doi: 10.1785/0120080264.

S. J. Lee, D. Komatitsch, B. S. Huang, and J. Tromp. Effects of topography on seismic wave propagation: An example from northern Taiwan. *Bull. Seismol. Soc. Am.*, 99(1):314–325, 2009b. doi: 10.1785/0120080020.

A. Legay, H. W. Wang, and T. Belytschko. Strong and weak arbitrary discontinuities in spectral finite elements. *Int. J. Numer. Meth. Eng.*, 64(8):991–1008, 2005. doi: 10.1002/nme.1388.

Q. Liu and J. Tromp. Finite-frequency kernels based on adjoint methods. *Bull. Seismol. Soc. Am.*, 96(6):2383–2397, 2006. doi: 10.1785/0120060041.

Q. Liu, J. Polet, D. Komatitsch, and J. Tromp. Spectral-element moment tensor inversions for earthquakes in Southern California. *Bull. Seismol. Soc. Am.*, 94(5):1748–1761, 2004. doi: 10.1785/012004038.

Y. Maday and A. T. Patera. Spectral-element methods for the incompressible Navier-Stokes equations. In *State of the art survey in computational mechanics*, pages 71–143, 1989. A. K. Noor and J. T. Oden editors.

R. Martin and D. Komatitsch. An unsplit convolutional perfectly matched layer technique improved at grazing incidence for the viscoelastic wave equation. *Geophys. J. Int.*, 179(1):333–344, 2009. doi: 10.1111/j.1365-246X.2009.04278.x.

R. Martin, D. Komatitsch, C. Blitz, and N. Le Goff. Simulation of seismic wave propagation in an asteroid based upon an unstructured MPI spectral-element method: blocking and non-blocking communication strategies. *Lecture Notes in Computer Science*, 5336:350–363, 2008a.

R. Martin, D. Komatitsch, and A. Ezziani. An unsplit convolutional perfectly matched layer improved at grazing incidence for seismic wave equation in poroelastic media. *Geophysics*, 73(4):T51–T61, 2008b. doi: 10.1190/1.2939484.

R. Martin, D. Komatitsch, and S. D. Gedney. A variational formulation of a stabilized unsplit convolutional perfectly matched layer for the isotropic or anisotropic seismic wave equation. *Comput. Model. Eng. Sci.*, 37(3):274–304, 2008c.

R. Martin, D. Komatitsch, S. D. Gedney, and E. Bruthiaux. A high-order time and space formulation of the unsplit perfectly matched layer for the seismic wave equation using Auxiliary Differential Equations (ADE-PML). *Comput. Model. Eng. Sci.*, 56(1):17–42, 2010.

E. D. Mercerat, J. P. Vilotte, and F. J. Sánchez-Sesma. Triangular spectral-element simulation of two-dimensional elastic wave propagation using unstructured triangular grids. *Geophys. J. Int.*, 166(2):679–698, 2006.

D. Michéa and D. Komatitsch. Accelerating a 3D finite-difference wave propagation code using GPU graphics cards. *Geophys. J. Int.*, 182(1):389–402, 2010. doi: 10.1111/j.1365-246X.2010.04616.x.

P. Monk and G. R. Richter. A discontinuous Galerkin method for linear symmetric hyperbolic systems in inhomogeneous media. *Journal of Scientific Computing*, 22-23(1-3):443–477, 2005. doi: 10.1007/s10915-004-4132-5.

C. Morency and J. Tromp. Spectral-element simulations of wave propagation in poroelastic media. *Geophys. J. Int.*, 175:301–345, 2008.

C. Morency, Y. Luo, and J. Tromp. Finite-frequency kernels for wave propagation in porous media based upon adjoint methods. *Geophys. J. Int.*, 179:1148–1168, 2009. doi: 10.1111/j.1365-246X.2009.04332.

S. P. Oliveira and G. Seriani. Effect of element distortion on the numerical dispersion of spectral element methods. *Communications in Computational Physics*, 9(4):937–958, 2011.

P. S. Pacheco. *Parallel programming with MPI*. Morgan Kaufmann Press, San Francisco, USA, 1997.

A. T. Patera. A spectral element method for fluid dynamics: laminar flow in a channel expansion. *J. Comput. Phys.*, 54:468–488, 1984.

F. Pellegrini and J. Roman. SCOTCH: A software package for static mapping by dual recursive bipartitioning of process and architecture graphs. *Lecture Notes in Computer Science*, 1067:493–498, 1996.

D. Peter, D. Komatitsch, Y. Luo, R. Martin, N. Le Goff, E. Casarotti, P. Le Loher, F. Magnoni, Q. Liu, C. Blitz, T. Nissen-Meyer, P. Basini, and J. Tromp. Forward and adjoint simulations of seismic wave propagation on fully unstructured hexahedral meshes. *Geophys. J. Int.*, 186(2):721–739, 2011. doi: 10.1111/j.1365-246X.2011.05044.x.

E. Priolo, J. M. Carcione, and G. Seriani. Numerical simulation of interface waves by high-order spectral modeling techniques. *J. Acoust. Soc. Am.*, 95(2):681–693, 1994.

W. H. Reed and T. R. Hill. Triangular mesh methods for the neutron transport equation. Technical Report LA-UR-73-479, Los Alamos Scientific Laboratory, Los Alamos, USA, 1973.

B. Rivière and M. F. Wheeler. Discontinuous finite element methods for acoustic and elastic wave problems. *Contemporary Mathematics*, 329:271–282, 2003.

G. Seriani and S. P. Oliveira. Optimal blended spectral-element operators for acoustic wave modeling. *Geophysics*, 72(5):SM95–SM106, 2007. doi: 10.1190/1.2750715.

G. Seriani and S. P. Oliveira. Dispersion analysis of spectral-element methods for elastic wave propagation. *Wave Motion*, 45:729–744, 2008. doi: 10.1016/j.wavemoti.2007.11.007.

G. Seriani and E. Priolo. A spectral element method for acoustic wave simulation in heterogeneous media. *Finite Elements in Analysis and Design*, 16:337–348, 1994.

G. Seriani, E. Priolo, and A. Pregarz. Modelling waves in anisotropic media by a spectral element method. In G. Cohen, editor, *Proceedings of the third international conference on mathematical and numerical aspects of wave propagation*, pages 289–298. SIAM, Philadephia, PA, 1995.

J. Tago, V. M. Cruz-Atienza, V. Étienne, J. Virieux, M. Benjemaa, and F. J. Sánchez-Sesma. 3D dynamic rupture with anelastic wave propagation using an hp-adaptive Discontinuous Galerkin method. In *Abstract S51A-1915 presented at 2010 AGU Fall Meeting*, San Francisco, California, USA, December 2010. www.agu.org/meetings/fm10/waisfm10.html.

C. Tape, Q. Liu, and J. Tromp. Finite-frequency tomography using adjoint methods - Methodology and examples using membrane surface waves. *Geophys. J. Int.*, 168(3):1105–1129, 2007. doi: 10.1111/j.1365-246X.2006.03191.x.

M. A. Taylor and B. A. Wingate. A generalized diagonal mass matrix spectral element method for non-quadrilateral elements. *Appl. Num. Math.*, 33:259–265, 2000.

J. Tromp, D. Komatitsch, and Q. Liu. Spectral-element and adjoint methods in seismology. *Communications in Computational Physics*, 3(1):1–32, 2008.

S. Tsuboi, D. Komatitsch, C. Ji, and J. Tromp. Broadband modeling of the 2002 Denali fault earthquake on the Earth Simulator. *Phys. Earth Planet. In.*, 139(3-4):305–313, 2003. doi: 10.1016/j.pepi.2003.09.012.

R. Vai, J. M. Castillo-Covarrubias, F. J. Sánchez-Sesma, D. Komatitsch, and J. P. Vilotte. Elastic wave propagation in an irregularly layered medium. *Soil Dynamics and Earthquake Engineering*, 18(1):11–18, 1999. doi: 10.1016/S0267-7261(98)00027-X.

K. van Wijk, D. Komatitsch, J. A. Scales, and J. Tromp. Analysis of strong scattering at the micro-scale. *J. Acoust. Soc. Am.*, 115(3):1006–1011, 2004. doi: 10.1121/1.1647480.

L. C. Wilcox, G. Stadler, C. Burstedde, and O. Ghattas. A high-order discontinuous Galerkin method for wave propagation through coupled elastic-acoustic media. *J. Comput. Phys.*, 229(24):9373–9396, 2010. doi: 10.1016/j.jcp.2010.09.008.

B. A. Wingate and J. P. Boyd. Spectral element methods on triangles for geophysical fluid dynamics problems. In A. V. Ilin and L. R. Scott, editors, *Proceedings of the Third International Conference on Spectral and High-order Methods*, pages 305–314, Houston, Texas, 1996. Houston J. Mathematics.

Appendix A

Troubleshooting

FAQ

Regarding the structure of some of the database files :

Question: Can anyone tell me what the columns of the SPECFEM2D boundary condition files in `SPECFEM2D/DATA/Mesh_canyon` are?

`SPECFEM2D/DATA/Mesh_canyon/canyon_absorbing_surface_file`
`SPECFEM2D/DATA/Mesh_canyon/canyon_free_surface_file`

Answer: `canyon_absorbing_surface_file` refers to parameters related to the absorbing conditions: The first number (180) is the number of absorbing elements (nelemabs in the code). Then the columns are:
column 1 = the element number
column 2 = the number of nodes of this element that form the absorbing surface
column 3 = the first node
column 4 = the second node

`canyon_free_surface_file` refers to the elements of the free surface (relevant for enforcing free surface condition for acoustic media): The first number (160) is the number of elements of the free surface. Then the columns are (similar to the absorbing case):
column 1 = the element number
column 2 = the number of nodes of this element that form the absorbing surface
column 3 = the first node
column 4 = the second node

Concerning the free surface description file, nodes/edges pertaining to elastic elements are discarded when the file is read (if for whatever reason it was simpler to include all the nodes/edges on one side of a studied area and that there are among them some elements that are elastic elements, only the nodes/edges of acoustic elements are kept).

These files are opened and read in `meshfem2D.F90` using subroutines `read_abs_surface()` and `read_acoustic_surface()`, which are in `part_unstruct.F90`